NICKEL-HYDROGEN CELL TEST PROGRAM SUMMARY

Vernon C. Mueller

McDonnell Douglas Astronautics Company - St. Louis Division

ABSTRACT

Three prototype 50 ampere-hour (AH) nickel-hydrogen cells of the Air Force Wright Aeronautical Laboratories (AFWAL) design have been cycled to failure by the McDonnell Douglas Astronautics Company-St. Louis Division (MDAC-STL). A summary of the life cycling tests and failure analyses of the cells are presented in this paper. The cells were cycled in a simulated low earth orbit regime at depths of discharge ranging from 25 to 80 percent. Trend data, such as end of discharge voltage and cell capacity, was recorded during test. Cells 1, 2, and 3 completed 17167, 2473, and 10080 charge/discharge cycles, respectively, prior to failure. All failed due to internal shorts, and were disassembled to determine cause of failure.

INTRODUCTION

Three NiH_2 cells rated at 50 AH were provided to MDAC-STL by AFWAL for a test program consisting of parametric tests followed by life cycling in a simulated low-earth orbit regime. Two of the cells had a zirconium-oxide, single-layer square weave separator (Cell 1/SN 104 and Cell 2/SN133), and the third had asbestos separators (Cell 3/SN148). All cells were manufactured in 1978 by Hughes Aircraft Company and contained Yardney positive electrodes made with a slurry process sinter and electrochemically impregnated. Figure 1 shows the cell general arrangement. MDAC-STL began the test program in November, 1979, concluding with failure of the last surviving cell in August, 1983. Test progress and interim results have been presented in earlier Goddard Space Flight Center Battery Workshops beginning in 1980. A summary of the life cycling tests and cell failure analyses are discussed in this paper.

During test, the cells were mounted horizontally in a fixture which gripped the cell about the cylindrical section and permitted heat to flow from the cell to the aluminum clamp and then to a supporting aluminum plate. Figure 2 shows the three cells in the test fixture. The one-inch aluminum baseplate was cooled by a circulating liquid coolant bath to provide temperature control of the cells. To assure that all heat was removed from the cells by conduction through the mounting clamp to the temperature controlled baseplate, insulation was applied completely around the cells. Temperature measured at a point on the side of the middle cell near the support fixture was used as the control point for temperature control.

LIFE CYCLING TESTS

Objectives of the cyclic tests were to obtain life data in a low-earth orbit regime and to identify and evaluate cell performance degradation. The cells were cycled by discharging into a fixed resistor such that the desired depth-of-discharge (DOD) was achieved in a 35-minute discharge period, followed by charging at approximately 50 amperes to a voltage limit, which was then held constant while the current tapered for the balance of the 55-minute charge interval. Cycling was controlled automatically to permit unattended operation. In order to prevent cell damage due to equipment malfunction, alarms were provided to shut down the test (open-circuit the cell) for over/under voltage, excessive discharge current, overtemperature, overpressure, and loss of facility power. At approximately 500 cycle intervals, cell capacity was determined by discharging at 25 amperes to a 1.0 volt cutoff. Capacity checks were accomplished immediately after a normal cyclic charge interval. Data was recorded at one-minute intervals during the capacity discharge and for one cycle at roughly 200 cycle intervals. For intervening cycles, data was recorded at 10-to 20-minute intervals as an aid to reconstruct anomalies, should they occur.

Cell 1 was cycled independently and Cells 2 and 3 were cycled in series. The control point temperature was set to 8°C for the first 2000 cycles, and to 23°C subsequently. Figure 3 shows energy removed on discharge as a function of cycles completed for these cells. The desired depth of discharge (DOD) for Cells 2 and 3 was 80 percent of rated capacity. However, this resulted in low end of discharge (EOD) voltage and DOD was reduced to 70 percent after 585 cycles. Further reduction occurred subsequently, again in response to low EOD voltage. Cell 1 DOD was reduced to 25 percent early in the test for 500 cycles to obtain data to support another study then in progress. It was then returned to 50 percent DOD to cycle 15706 at which time it was reduced due to low EOD voltage.

Cycling test trend data is shown in Figures 4 and 5. Cell 2 had recurring problems with low EOD voltage. At cycle 2473, cycling was stopped to perform a capacity check. Following the capacity check, Cell 2 failed to recharge. Three days later, a 5-ampere charge was again attempted, but Cell 2 failed to respond. Apparently an internal short had developed and the cell was removed from test. Cells 1 and 3 continued to cycle with relatively few problems. Degradation of EOD voltage and reduction of measured capacity was observed, as noted in Figures 4 and 5. Cell 3 failed abruptly after completing 10,080 charge/discharge cycles. Evidently, a massive short had developed, as evidenced by a high cell temperature. At this point, the cell was disconnected electrically, but physically left in the test fixture.

Cell 1 lost a significant portion of its hydrogen gas when a leak developed in a pressure fitting, which attached a pressure transducer to the cell at Cycle 6229. The loss of hydrogen caused shutdown of Cell 1 cycling due to an undervoltage alarm during discharge. During investigation of the failure, the cell was shorted for several weeks. The leak in the external plumbing was corrected and the cell was backfilled with 50 psi of hydrogen several times to replenish the cell. When the cell was recharged, it showed good voltage recovery and was returned to cycling. As shown in Figure 4, the reconditioning effect on EOD voltage was soon diminished and remained relatively stable for several thousand cycles after the anomaly occurred.

At Cycle 11891, Cell 1 was inadvertently overcharged for 20 hours, with a total input energy of 118.4 ampere-hours due to an equipment malfunction. There was no apparent cell damage; therefore, the cell was returned to cycling after equipment repair. The effect of this long overcharge can be seen in the increase in measured capacity after Cycle 12015. Measured capacity was 59 ampere-hours at this point.

Cell EOD voltage was degrading on Cell 1 at approximately 15,000 cycles. The charge limit voltage was increased slightly, but the voltage continued to degrade and an undervoltage alarm caused shut down at Cycle 15690. At this time, the cell was recharged and a capacity check was performed. Measured capacity was only 23.9 ampere-hours, so the discharge energy was reduced from 25 to 15 ampere-hours. The effect on EOD voltage is reflected in Figure 4. As shown in Figure 5, measured capacity improved considerably after the low reading of 23.9 ampere-hours. Reasons for the behavior are not known. Cycling continued smoothly until failure occurred at Cycle 17168. Failure occurred about 20 minutes into the discharge of Cycle 17168 and was accompanied by a high-cell temperature pulse.

FAILURE ANALYSES

Each of the cells was dissected to determine the cause of failure. A dry nitrogen purge was used prior to disassembly to eliminate any residual hydrogen. Then the cell was cut open with a lathe just below the weld toward the negative terminal (see Figure 1). The negative end of the pressure vessel was then removed, exposing the electrode stack assembly. Figure 6 is a sketch of the electrode stack assembly. For purposes of identification, the electrodes are numbered consecutively from the positive end of the cell (weld ring end). Elements of the electrode stack assembly were removed individually, and photos, observations, etc. were accomplished as the disassembly progressed.

CELL 2

Cell 2 (SN 133) failed after 2473 charge/discharge cycles. This cell had a Zircar separator. Cells 2 and 3 were connected in series during cycling, and were discharged in series during a capacity check after 2473 cycles. Cells 2 and 3 delivered 27.3 and 46.9 ampere-hours to a one-volt cutoff, respectively. The discharge characteristic for Cell 2 showed a second voltage plateau at approximately 0.85 volts, and the continuing discharge of Cell 3 drove Cell 2 into reversal at -0.06 volts. It remained reversed for 14 minutes until Cell 3 reached one volt. After the discharge, Cell 2 remained at an open-circuit voltage of 0.004 volts for three days before a five-ampere recharge was attempted and the voltage failed to recover.

After Cell 2 was cut open and the polysulfone nut was removed to free the stack, a voltage measurement of 0.908 volts was observed indicating that the short was removed as electrode stack compression was relieved. Disassembly of the electrode stack revealed no obvious evidence of a mechanical short. Three anamolous areas were found where active material had bridged through burnholes from a positive electrode to an adjacent negative. If this material

was conductive, it could have provided a shorting path when the stack was tightly compressed. Tests by Hughes Aircraft Company have shown that such a bridge will remain nonconductive for at least 1500 cycles. If these anomalies were formed early enough for sufficient positive material to be reduced to conductive nickel, it would account for the condition. This seems the most likely failure mechanism. Numerous gas screens and negative electrodes had tiny burn holes randomly spaced due to rapid oxygen recombination (popping). The damage was most noticeable on the gas screens and the teflon surface of the negative. However, this phenomenon was not a contributing factor to the observed failure.

CELL 3

Cell 3 (SN 148) completed 10,080 charge/discharge cycles prior to failure. Cell failure analysis was discussed in detail at the 1983 Battery Workshop. Therefore, this discussion will be somewhat abbreviated. At approximately five minutes into the charge period of cycle 10,080, a cell overtemperature was sensed and, on the next data scan a few seconds later, the voltage was less than 0.5 volts. The automatic circuitry open-circuited the cell. When the next data set was recorded 18 minutes later, the highest temperature was 89.6°C, measured at the top of the cylindrical section furthest removed from the coolant bath. Intermediate data points were not recorded, and the peak temperature excursion is not known. The cell was disconnected electrically after failure, but physically left in the test fixture for approximately 11 months before the failure analysis was done.

Something loose could be heard rattling within the pressure vessel prior to dissection. After the negative end of the pressure vessel was removed, the ceramic insulating washer at the negative terminal was found broken into four pieces, which accounted for the rattling noise. The shoulder at the end of the polysulfone core had fractured completely around the intersection with the central part of the core. This allowed the electrode stack to relieve, leaving the first negative roughly flush with the broken end of the polysulfone core. The shoulder, belleville washer, and honeycomb end plate were loose on the negative leads. The reservoir had melted completed acróss the annular section in the area of the negative tab and the electrode stack was indented. Forces applied to the plates by the negative tabs when the stack relieved may have caused this indentation.

The electrode stack assembly was disassembled, element by element. Shorting of adjacent positive and negative plates was found at the inner perimeter of the plates in the area of the negative tab. In many cases, active material from the positive plate was imbedded in the adjacent negative. Gas screens and reservoirs between negative and positive plates had melted and shrunk and were fused to the teflon-coated side of the negative electrodes. Damage was observed to extend from the negative end of the electrode stack to plate set 27, with the most extensive damage seen in plate sets 34 to 37. The heat pulse generated when the shorting occurred appeared to discolor and swell the polysulfone core, such that a ribbed appearance was created and a black deposit was left where the positive plates restricted this swelling. The dimension from the end of the core to the first indentation caused by a positive plate

was less than the combined thickness of the end plate and belleville washer, which implies that the end of the core fractured prior to the occurrence of the short. Positive plate thicknesses were measured during disassembly and, assuming each was fabricated at the maximum dimension, electrode stack height increased 0.395 inches during cycling.

We have concluded that positive plate growth during cycling was the primary reason for cell failure. A chronological history of the failure can be postulated as follows:

- Positive plate growth during cycling causes fracture of the shoulder from the polysulfone core.
- Forces applied to the electrodes when the stack expands creates pressure points between adjacent pairs of electrodes, most pronounced at the tab attachments.
- A short occurs at a pressure point after some period of time.
- The heat pulse and mechanical forces generated by the short cause the failure to propagate to adjacent plate sets.

CELL 1

Cell 1 (SN 104) completed 17,167 charge/discharge cycles prior to failure. Failure occurred on 23 August 1983, at about 20 minutes into discharge of cycle 17,168. Cycling was terminated by an undervoltage alarm which open-circuited the cell, but it continued to self-discharge and heat up. The bottom of the cell reached 183°C seven minutes after shutdown, indicating a short circuit. At thirty minutes after failure, cell temperature was 115°C. During an automatic shutdown, active cooling is terminated. An hour after shutdown, the voltage had dropped to zero and the pressure fell to approximately 100 psi. A five-ampere, five-minute recharge was attempted without success. The cell was left in the test fixture until the failure analysis was begun on 17 October 1983.

On the basis of our failure analysis of Cell 3, we decided to X-ray Cell 1 prior to disassembly to determine whether a similar condition existed. Inspection of the radiographs showed the belleville washer and end plate were free and that the electrode stack assembly had relieved. Also, loose parts could be heard rattling inside the pressure vessel.

The ceramic washer from the negative terminal was found fractured into five segments inside the cell when the negative end of the pressure vessel was removed, which caused the rattling noise. Again, the shoulder of the polysulfone core had fractured completely around the intersection with the core. The shoulder, end plate, and belleville washer were retained by the negative leads. The electrode stack had relieved with the first negative electrode extending slightly past the fractured end of the core. Also the

electrodes were indented along an axis corresponding to the axis in which the plate tab to positive and negative leads is made. This depression is believed to have been caused by forces exerted through the leads when the stack relieved. Figure 7 is a view of the electrode stack prior to disassembly showing the indentation. Also, the negative reservoir had shrunk and necked in at one point, probably due to heating. Visual examination of the fractured end of the core showed striations similar to that seen in fatigue failure of metals.

An electrode-by-electrode disassembly revealed shorting of adjacent positive and negative plates at the inner perimeter of the plates in the area where the negative leads attach. Active material from the positive plate was imbedded in the adjacent negative in many cases. Also, the gas screen between negative and positive plates had melted and shrunk and was fused to the teflon coated side of the negative plate. Most severe damage to the gas screen was at a point where shorting had occurred at the negative lead to plate attachment. As the gas screen shrunk, it apparently fused to the outer periphery of the negative plate and peeled the teflon backing away from the underlying screen structure. Figure 8 is a photograph of negative plate 35 showing active material from positive plate 34 imbedded at the inner periphery where the negative lead attaches to the tab. Note also how the gas screen peeled back the teflon coating as it shrank due to heating. Gas screen shrinkage, melting, and fusing to the negative plate, and shorting of positive and negative electrodes extended throughout the stack assembly. Pin holes were found in many of the negative plates, indicating that "popping" occurred. As disassembly progressed toward the positive end of the electrode stack assembly, the plates became more planar.

Examination of the polysulfone core after disassembly showed the discoloration and swelling which is apparently caused by the heat pulse generated when shorting occurs. Figure 9 shows the polysulfone core attached to the positive hemisphere after the electrode stack elements have been removed. The degree of discoloration is believed to be proportional to the heat generated at that point. Applying that premise, the short is believed to have occurred first at a point approximately one-third of the stack thickness from the positive end and progressed outward in both directions. The swelling of the core causes a ribbed appearance and a black deposit is left where the positive plates restrict the swelling. The dimension from the fractured end of the core to the first indentation caused by a positive plate is less than the combined thickness of the end plate and belleville washer, which implies that the shoulder fractured from the end of the core prior to the occurrence of the short.

Positive plate thicknesses were measured during disassembly and ranged from 0.038 to 0.048 inches. Assuming that each positive plate was fabricated at the maximum dimension of 0.032 inches, the thickness of the electrode stack assembly increased by 0.451 inches during cycling. the cell failed in a nearly identical manner to Cell 3, and we believe the failure history was also the same. Positive plate growth of this magnitude cannot be accommodated; and, after the stack relieves, a short occurs at a pressure point between adjacent pairs of electrodes which ultimately results in the massive internal damage observed.

CONCLUSIONS

The prototype cells tested do not exhibit the cyclic life necessary for spacecraft power systems operating in low-earth orbit. However, when one considers the high depth of discharge used for the cyclic tests, the performance of Cell 3/SN148 and Cell 1/SN 104 are certainly respectable as compared to nickel-cadmium cell life. Cells used for these tests are prototypes, and do not represent a mature technology. Also, considerably more data needs to be acquired to obtain a statistically significant data base for low-earth orbit applications. The most significant cause of failure is the positive plate growth experienced with these early design positive electrodes. More recent positive electrodes show significantly less growth with cycling, and should retard or eliminate the type of failure seen in Cells 1 and 3. Testing of current generation cells incorporating the improved positive electrodes, as well as other design improvements, are required to obtain necessary cyclic life data. MDAC-STL plans to test a 21-cell, nickel-hydrogen battery in a simulated low-earth orbit regime in the near future.

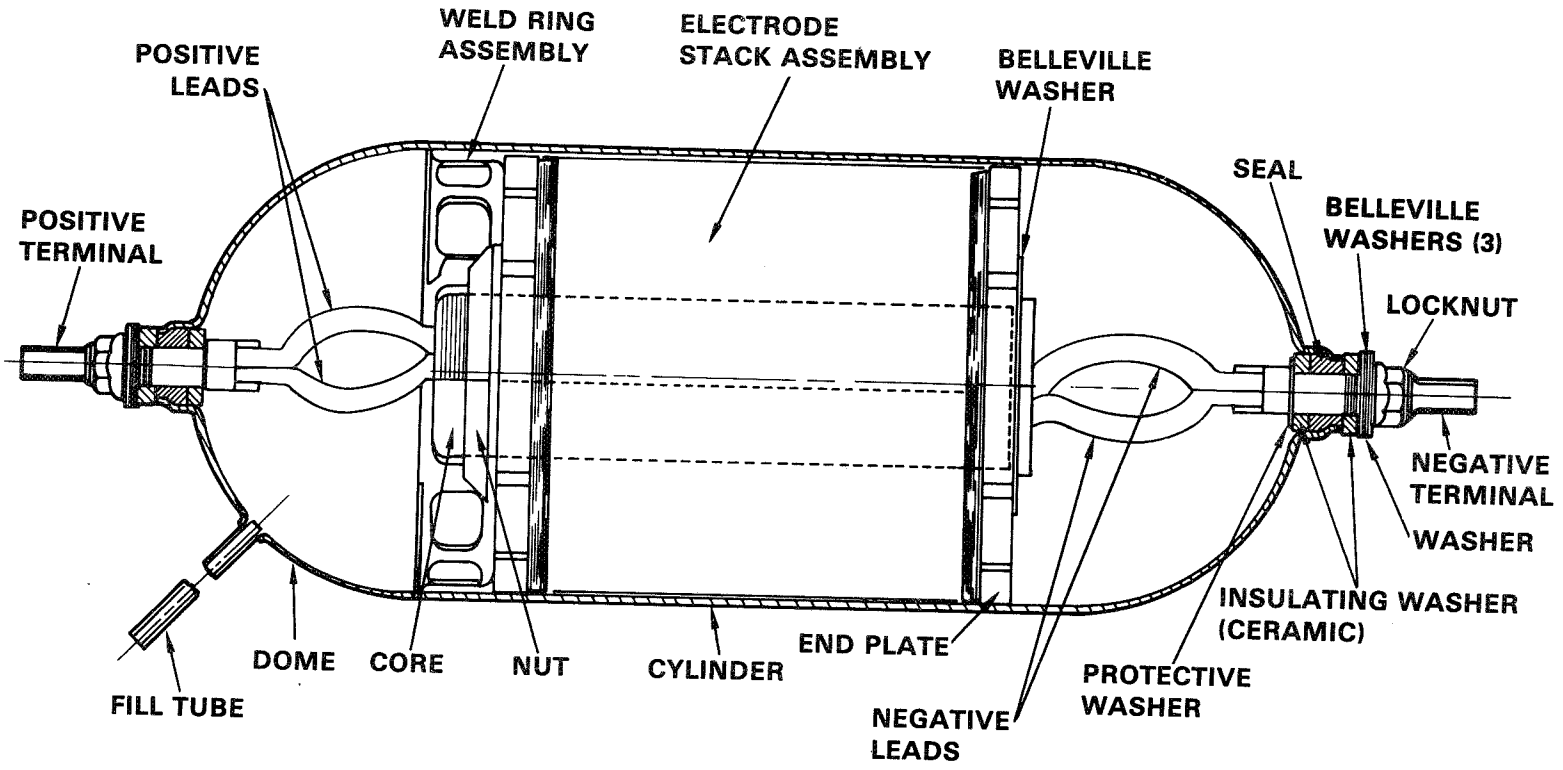

Figure 1. 50 Ampere-Hour Nickel-Hydrogen Cell

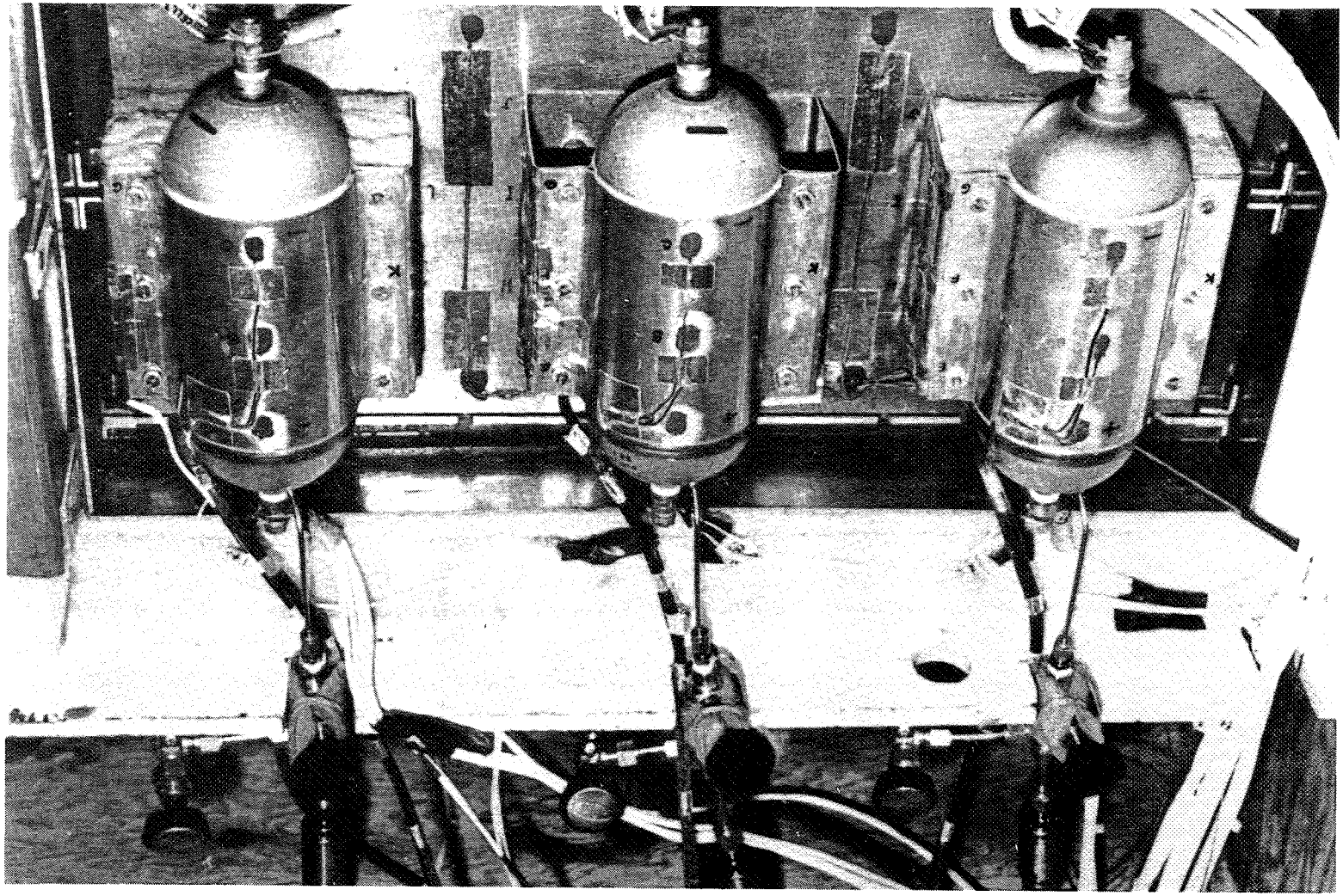

Figure 2. Nickel-Hydrogen Cells Mounted in Test Fixture

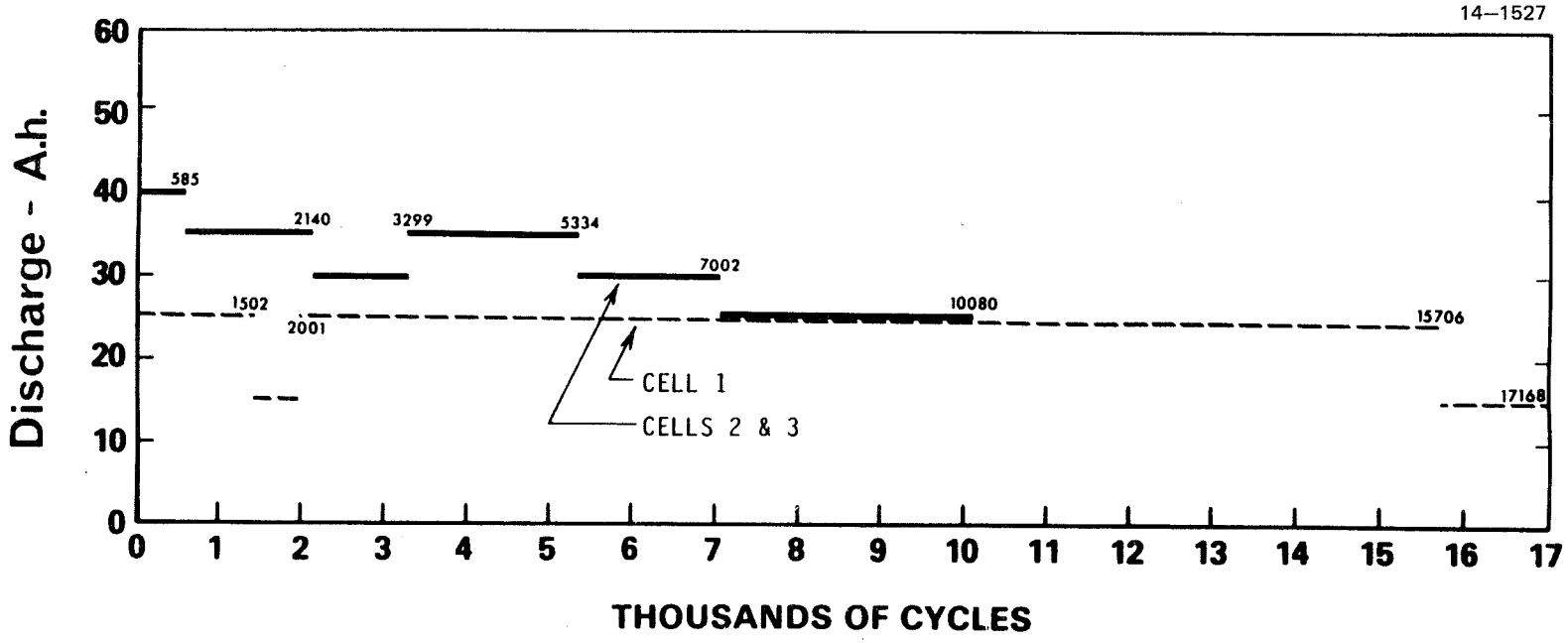

Figure 3. Discharge versus Cycles

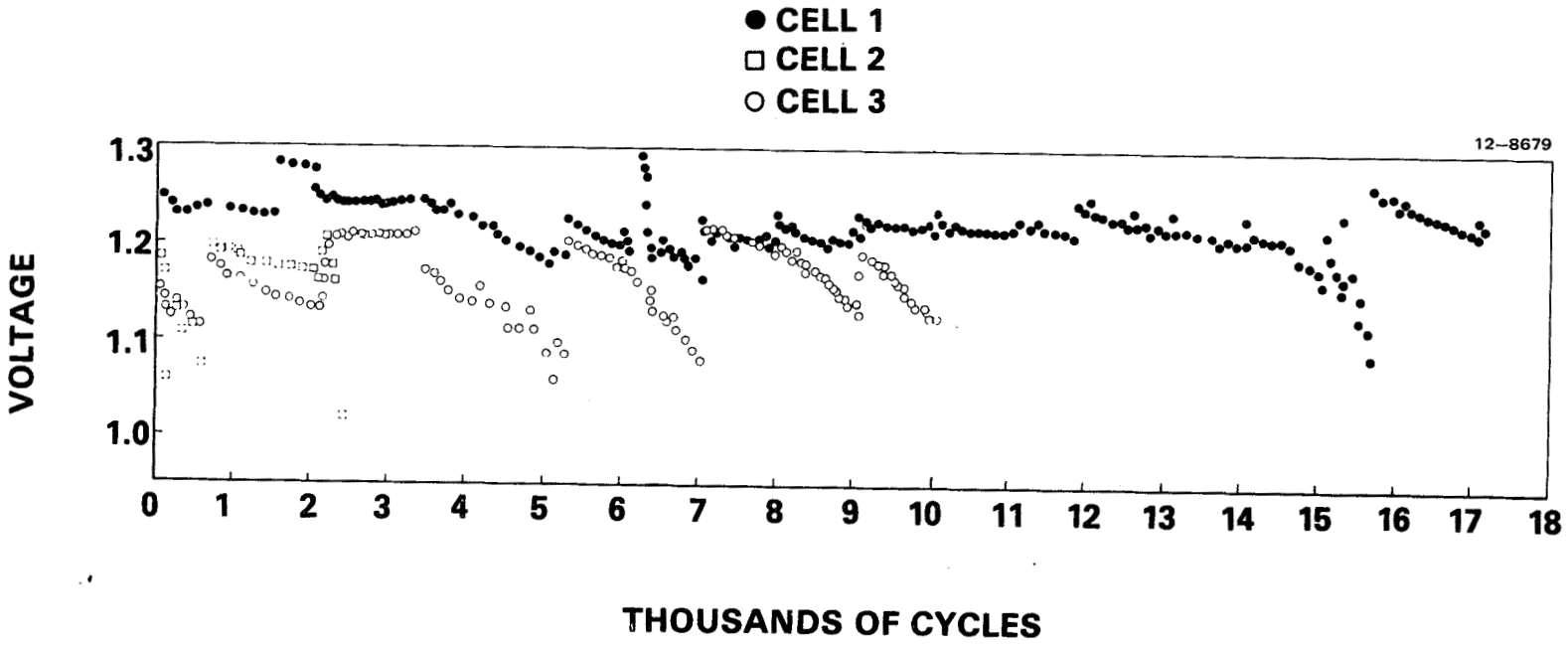

Figure 4. Cell End-of-Discharge Voltage versus Cycles

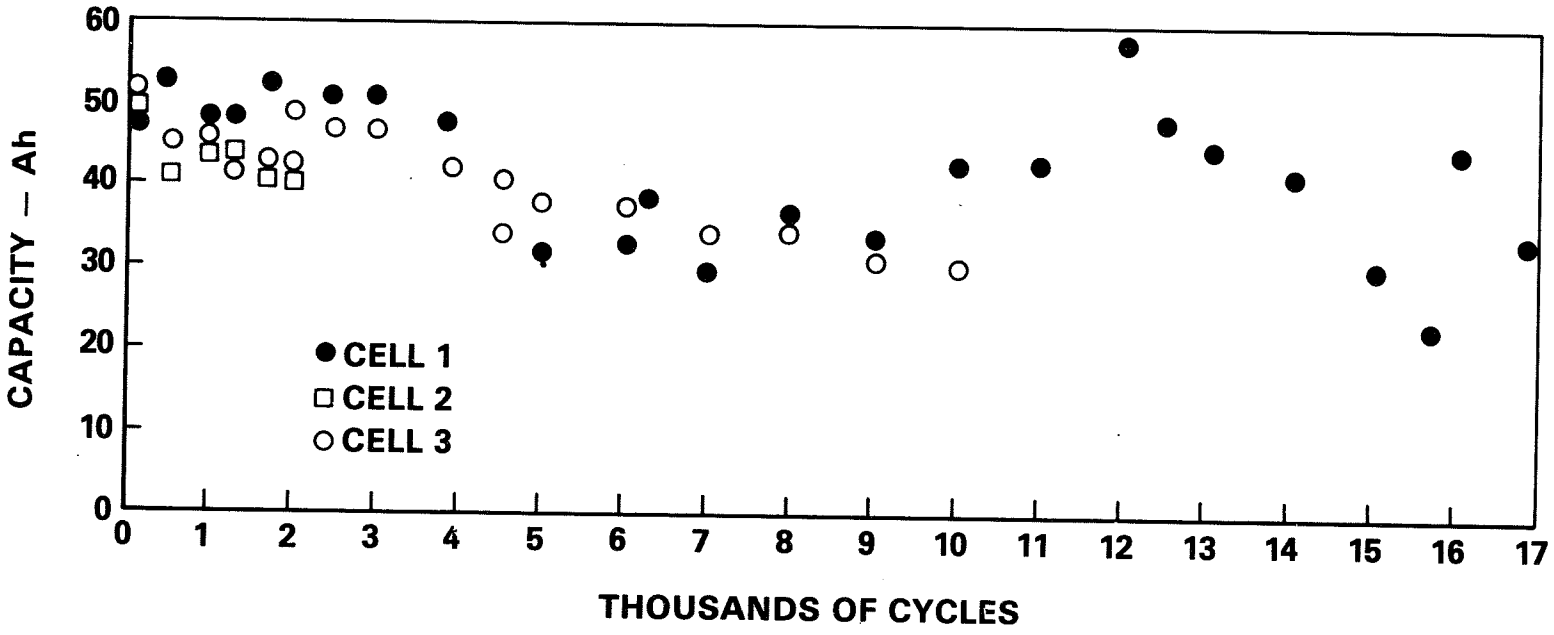

Figure 5. Cell Measured Capacity versus Cycles

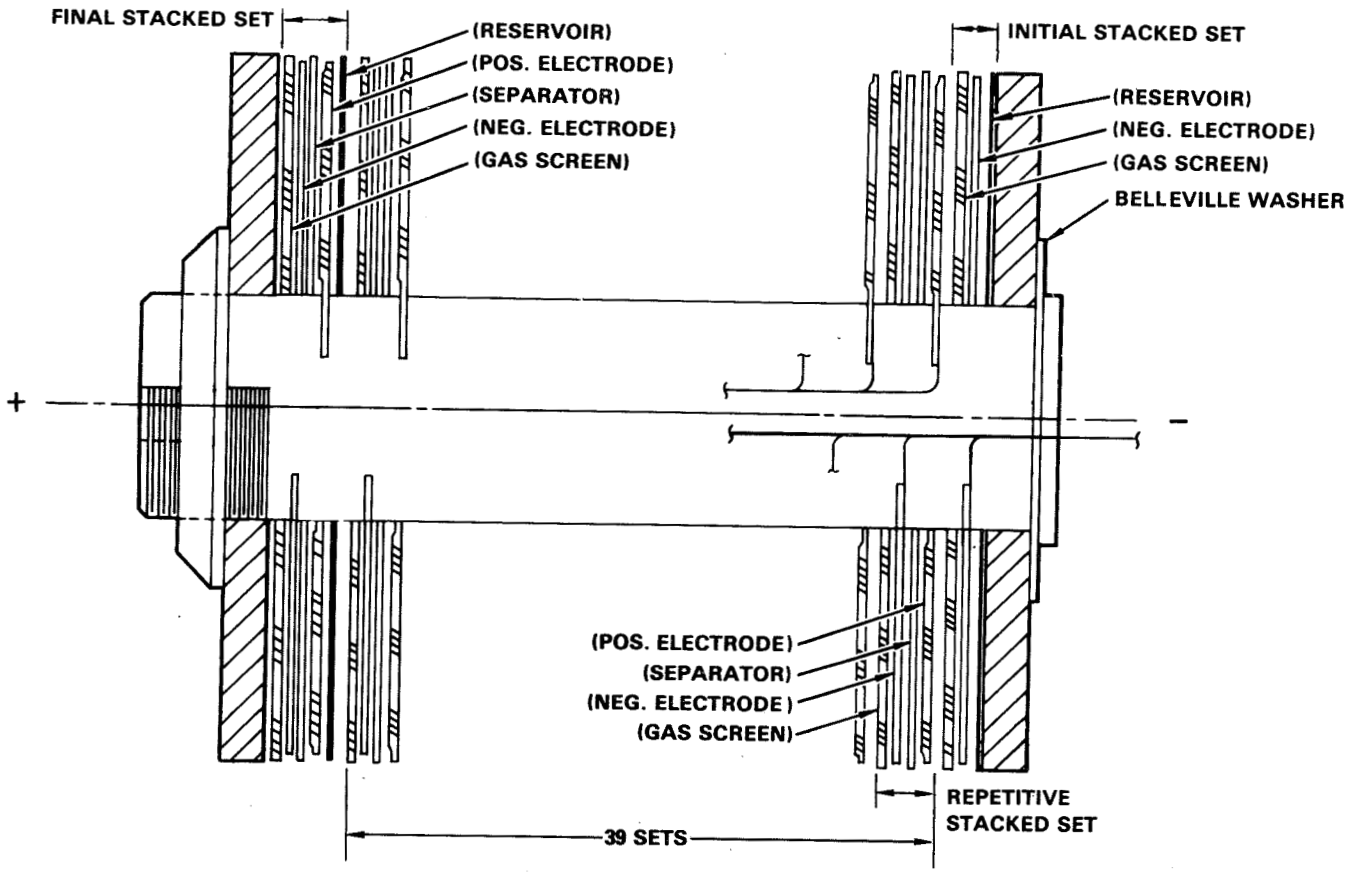

FIGURE 6

Figure 6. Electrode Stack Sketch

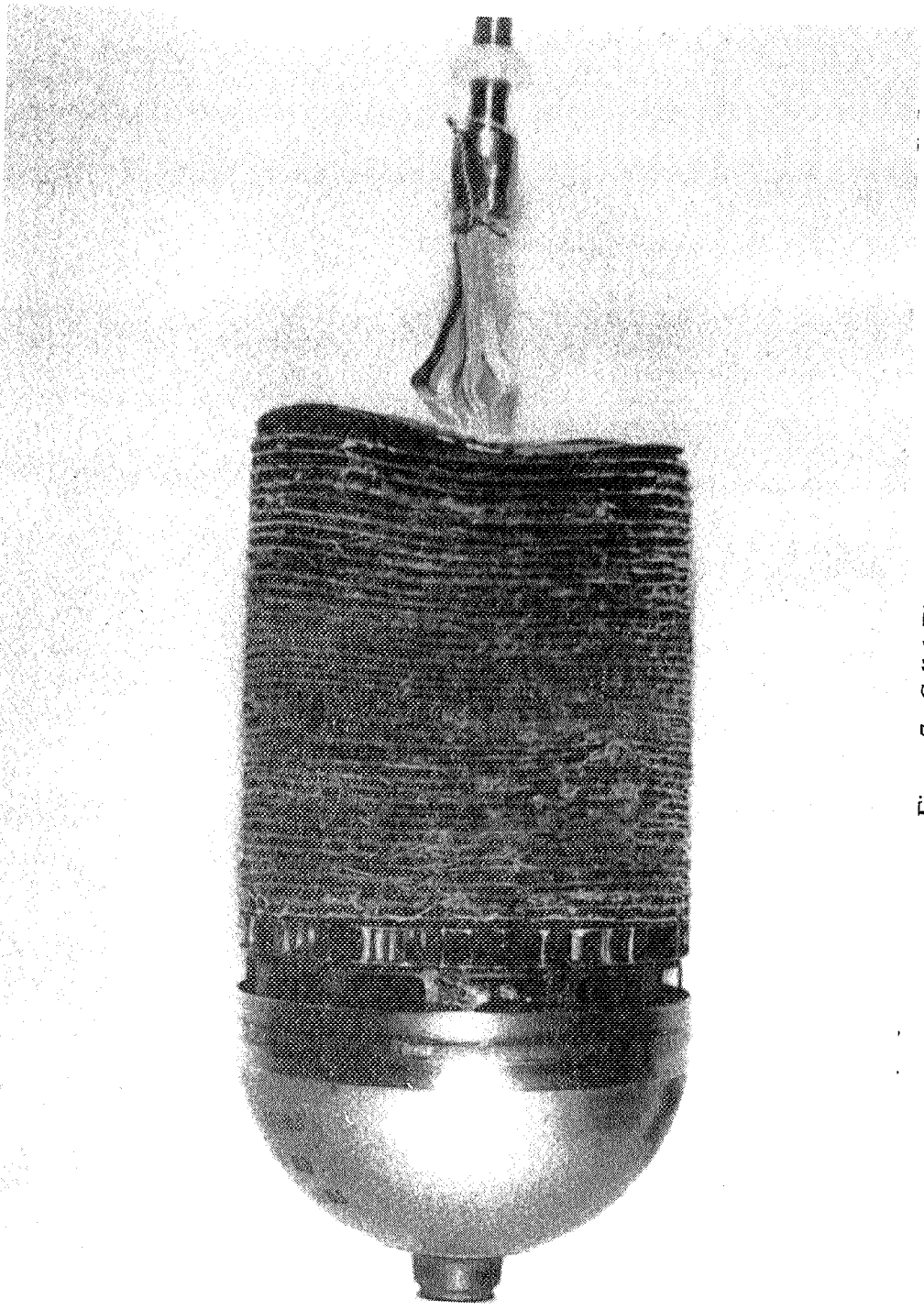

Figure 7. Cell 1 Electrode Stack Assembly

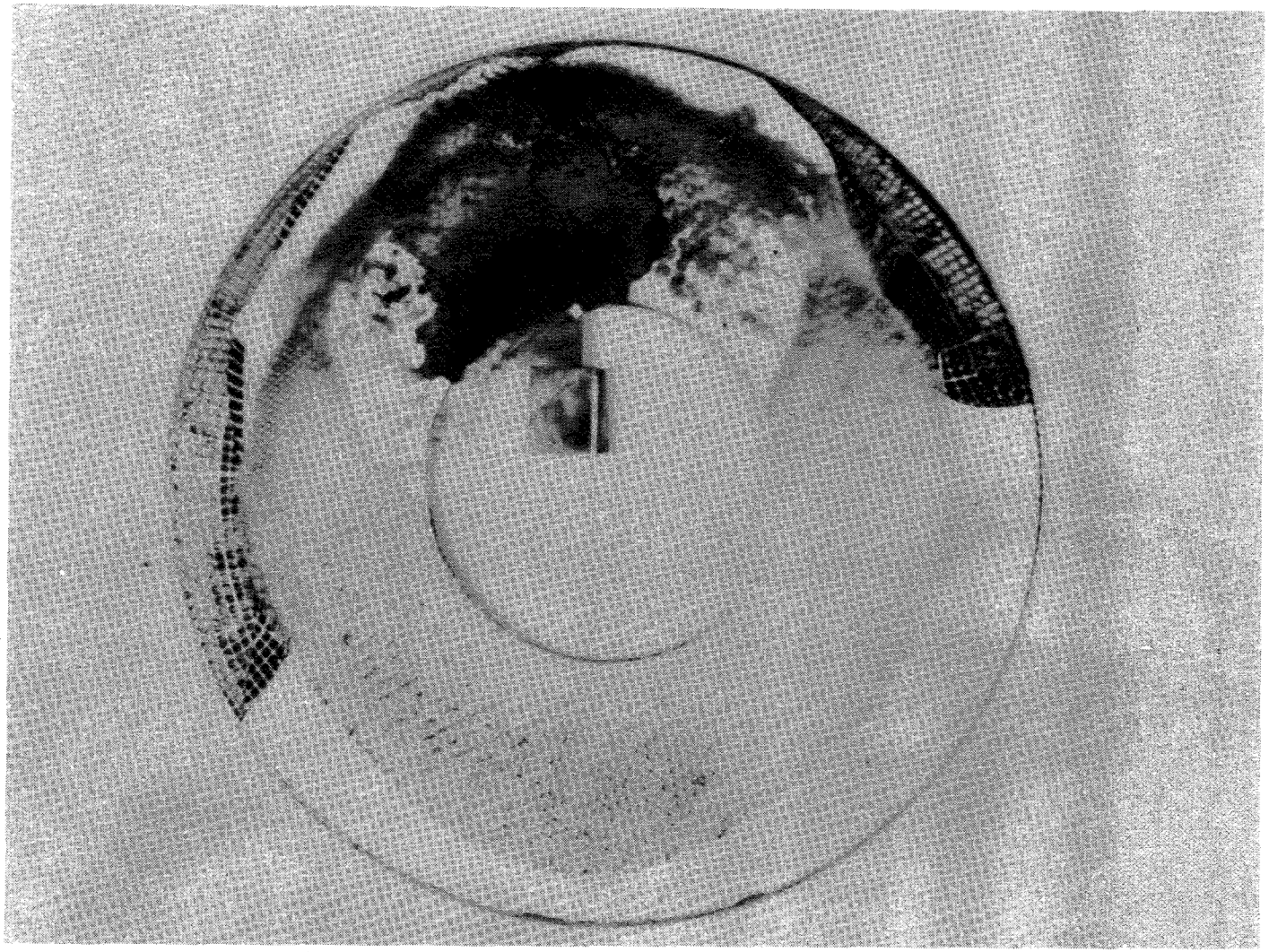

Figure 8. Cell 1 Negative Plate 35 and Gas Screen

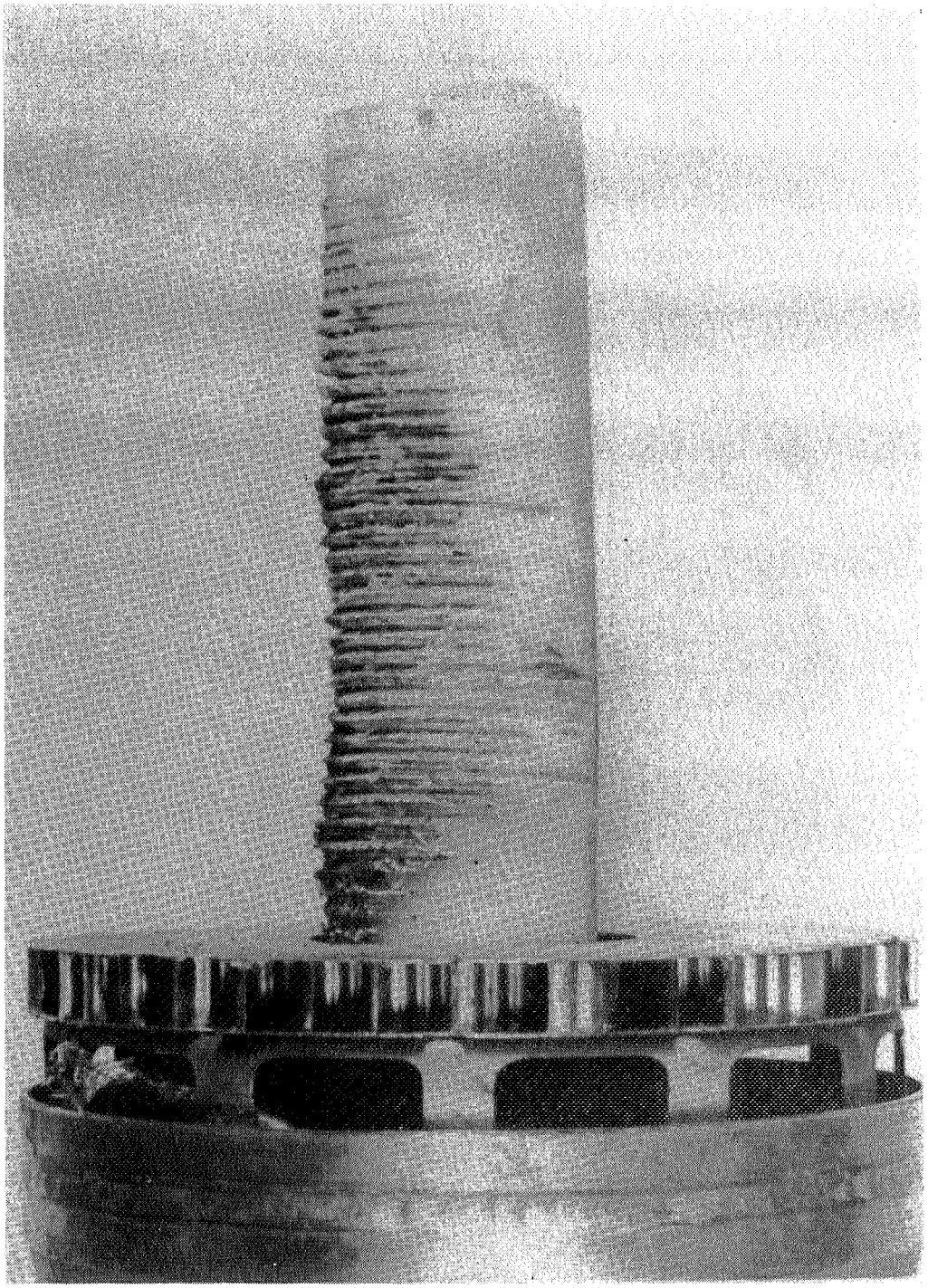

Figure 9. Cell 1 Polysulfone Core